 CMES, vol.104, no.6, pp.471-491, 2015

Numerical Simulation of An Experienced Farmer Lifting Tubers of Cassava for Designing A Bionic Harvester

Wang Yang[1,2], Juanjuan Li[1], Jian Yang[1,3] and Lin Wei[4]

Abstract: Harvesting is the most difficult and costly operation in cassava production. Currently, most cassava harvest still depends on manual tools. Effective mechanized harvesters are necessary to improve harvesting quality and reduce production cost. Therefore, it is very important to figure out key information for designing an effective tuber lifting system used in bionic "dig-pull" harvesters. A numerical simulation model of human-stem-tuber-soil system was developed to carry out numerical simulation of manually pulling tuber. Coupling algorithm of Lagrange and smoothed particle hydrodynamics (SPH) was used in the model. Lifting mechanism of experienced farmer was studied at a micro level. Influence of lifting velocities was discussed. The results show that when the soil volume was compressed by 5% in the lifting direction, a ring sheared surface of soil occurs. The soil is gradually sheared and fractured along with the surface during lifting. After that, the soil falls down on ground due to tuber jittering and completely detaches from the tuber. Large lifting velocity, resulting in high harvesting efficiency, but consumption of energy also increases. Before the height achieves 75 mm, higher velocity is beneficial for improving efficiency, but after that, lifting velocity should be appropriate to avoid tuber broken and lost.

Keywords: cassava tuber, numerical simulation, lifting mechanism, influence of velocity, bionic harvester.

1 Introduction

Cassava is a tuber crop that is widely planted in tropical and subtropical regions. It is the fourth largest crop, after wheat, rice, and maize for food feeding over 600

[1] College of Mechanical Engineering, Guangxi University, Nanning 530004, China.
[2] Guangxi Key Laboratory of Manufacturing System & Advanced Manufacturing Technology, College of Mechanical Engineering, Guangxi University, Nanning 530004, China.
[3] Corresponding author. E-mail: gxuyangjian@163.com; Tel: +86-13557014056
[4] Department of Agricultural and Biosystems Engineering, South Dakota State University, Brookings 57007, USA.

million people in the world. Because of the way cassava tubers (named tuber) grow, harvesting is the most difficult and costly operation in cassava production. Currently, most cassava harvest still depends on various manual tools for field operations. Those methods are inefficient and uneconomic due to expensive labor costs and a considerable amount of tubers either remaining in the ground or damaged, which are highly susceptible to decay or change to oxidation dark color, resulting in large value losses [Kolawole, Agbetoye and Ogunlowo (2010)]. Therefore, effective mechanized cassava harvesters are necessary to improve harvesting quality and production cost. Currently, "dig-pull" style method is the main approach used in mechanized harvesters. In this method, during cassava harvesting, the soil around tubers was dug first and then the stem was pulled up to lift out the tubers by a lifting device on the harvester. If the soil hardness is low, the tubers would be lifted directly. During tubers lifting, they may be broken off easily if the lifting velocity is improper, which lead to low harvesting quality and tuber losses [Agbetoye (1999)]. Thus, fully understanding the tuber lifting mechanism and influence of lifting velocity is critical for designing an effective tuber lifting system for an efficient "dig-pull" cassava harvester. It is found that different tuber lifting velocities result in different harvesting quality during manually harvesting. Experienced farmers have 30-35% higher efficiency and 20-30% lower loss rate than those of non-experienced farmers during cassava harvesting. Therefore, based on mechanism of manually pulling tubers and lifting velocities, it may be a good way to explore useful information for determination of optimal velocity model used in the design of an effective tuber lifting system for bionic "dig-pull" cassava harvester.

In 1980s, a "dig-pull" cassava tuber harvester was developed by the University of Leipzig in Germany. During harvesting, a digging shovel can dig and loose the soils around tubers and then a clamp lifts up and transports the tubers to a conveyor on the harvester. Although harvesting efficiency of this harvester was improved, the harvesting loss still remained large due to lack of information for the proper lifting velocities of the tuber lifting mechanism [Bobobee, Okyere, Twum, Neumann and Knechtges (1994)]. Many efforts are made to address this harvesting quality issue. After modified the harvester design, another "dig-pull" cassava harvester called "Chm-3407" was developed by the Estonia Company [Et Moisakula Ltd, Estonia]. Yulan Liao et al. (2012) designed a new digging shovel, a clamping conveyor, and a power transmission device for improving cassava tuber harvesting quality [Liao, Sun, Liu, Cheng and Wang (2012)]. LAS Agbetoye et al. (2000) established a lifting force model for the analysis of lifting a flat board buried in soil using mechanical methods. Although this model was able to predict actual force closely for the case of a simple flat board, there are still many limitations in the model for analyzing a complicated tuber system [Agbetoye, Dyson and Kilgour

(2000)]. Yang et al. (2011a) developed a mechanical and mathematical model of lifting force on tuber to investigate the linkages between lifting speed, lifting force, tuber variation, and soil conditions for tuber harvesting quality improvement by integrating physical tests, mechanical analysis, and numerical simulation method [Yang, Cai, Yang and Huang (2011)].

Nonetheless, interaction between tubers and soils, stress variation and deformation of tuber, the deformation and fracture of soil, and the mechanism of soil separating from tubers during manual tubers lifting still remain challenge. This has been a "bottleneck" for designing efficient tuber lifting systems for bionic "dig-pull" cassava harvesters.

Tuber lifting mechanism is complicated. It is difficult to fully understand the interaction between tuber and soil, stress variation and deformation of tuber, the deformation and fracture of soil, and the mechanism of soil separating from tubers by physical experiments. Numerical simulation method is an effective method that can be used to study scientific questions at a micro level. In the numerical simulation methods, the large deformation of a material couldn't be simulated by Lagrange method that has the advantages of less calculation time and mature boundary processing algorithm. But Smoothed Particle Hydrodynamics (SPH) method is one of typical non-mesh Lagrange method and the discretization of which uses the movable points of fixed mass instead of mesh. It can be used to solve large deformation simulation of the fracture of continuum structures and the rupture of brittle solid slabs, for example, a steel ball penetrating a thin steel plate; fracture of brittle solids; metal forming; material cutting processing; frictionless contact; flow in screw extrusion; fluid structure interaction [Seo, Min and Lee (2008);Benz and Asphaug (1995); Cleary, Prakash and Ha (2006); Limido, Espinosa, Salaun and Lacome (2006); Vignjevic, De Vuyst and Campbell (2006); Dong , Liu, Jiang, Gu, Xiao, Yu and Liu (2013); Messahel and Souli (2013)]. Lagrange and SPH method have their own characteristics. To combine the advantages of them, Johnson (1994) firstly proposed a coupled algorithm of Lagrange and SPH method and used it to study penetration problems [Johnson (1994)]. Currently, the coupling algorithm has been applied in many fields. The behavior of a floating structure and the structural response to water impact was studied by using the coupling algorithm [Campbell, Vignjevic, Patel and Milisavljevic (2009)]. A coupling calculation model of reinforced concrete was established and applied in the simulation of a projectile's impact on a slab [Caleyron, Chuzel-Marmot and Combescure (2009)]. The response of buried structure in soil subjected to blast load was studied by using the coupling algorithm [Lu, Wang and Chong (2005)]. Simulation of abrasive water jet machining was studied by using the coupling algorithm [Wang, Gao, and Gong (2010)]. Impact dynamics simulation was also studied by using the coupling algo-

rithm [Zhang, Qiang and Gao (2011)]. Simulation of violent fluid-structure interaction was investigated by using the coupling algorithm [Fourey, Oger, Le Touz'e and Alessandrini (2010)]. A coupling calculation model of a shovel digging operation for "dig-pull" cassava tuber harvesters was developed to carry out numerical simulations of loosening soil using the coupling algorithm as well [Yang, Yang, Jia, Wang and Huang (2013)]. These previous studies show that, soil large deformation simulation of interaction between tubers and soils can be solved effectively using the coupling algorithm. The presenting study aims to study lifting mechanism of experienced farmer in manually pulling harvest and influence of lifting velocities using the Lagrange and SPH coupling model and numerical simulations. The study outcomes will provide useful information for determination of optimal velocity model that can be used in the design of lifting mechanical systems for bionic cassava tuber harvesters.

2 Materials and Simulation Methods

A variety of cassava (named South-China 205), shown in figure 1, is used as the main study object in this research. This cassava is widely planted in China. The cassava cultivated farm is in Wu Ming, Guangxi province, which is the largest cassava cultivated farm in China. A numerical simulation model of human-stem-tuber-soil system will be established using the coupling algorithm of Lagrange and SPH method. Based on the numerical simulation models, lifting mechanism of experienced farmers in manually pulling harvest and influence of lifting velocities on lifting force and effective stress of tuber will be studied to provide helpful information and evidence for designing a tuber lifting system used in bionic "dig-pull" cassava harvesters.

Figure 1: Growth situation of cassava.

2.1 Coupling algorithm of SPH and Lagrange

SPH method is one of numerical methods that can be used to solve partial differential equation. Firstly, it discretizes the solution domain of the equation, and then an approximate equation is used to represent field functions and their derivatives at any point. Partial differential equations are transformed into a series of discretized ordinary differential equations which are only related to time. After that, the ordinary differential equations are solved to obtain the numerical solution using traditional numerical methods.

The formulation of SPH is often divided into two key steps. The first step is the integral representation, the so-called kernel approximation of field functions. The second one is the particle approximation [Liu and Liu (2005); Hallquist (2006)].

(1) Kernel approximation

In SPH method, the integral formula of a function $f(x)$ can be written as

$$f(x) = \int_{\Omega} f\left(x'\right) \delta\left(x - x'\right) dx' \tag{1}$$

Where$\Omega$is computational domain, x is coordinate vectors, and $\delta(x - x')$ is Dirac delta function.

The Dirac delta function in formula (1) is replaced by kernel function $W(x - x', h)$, and the integral approximate formula is

$$\langle f(x) \rangle = \int_{\Omega} f\left(x'\right) W\left(x - x', h\right) \mathrm{d}x' \tag{2}$$

Where:$h$is the smoothing length of the kernel function.

(2) Particle approximation

The particle approximation formula of function $f(x_i)$ is given by

$$\langle f(x_i) \rangle = \sum_{j=1}^{N} \frac{m_j}{\rho_j} f(x_j) W_{ij} \tag{3}$$

Where m_j and ρ_j are the mass and density of the particle j, respectively. N is the number of particles in the support domain of particle i. Here W_{ij} is a B-spline based on smoothing function with radius $2h$, and

$$W_{ij} = W(\boldsymbol{x}_i - \boldsymbol{x}_j, h) = W\left(\left|\boldsymbol{x}_i - \boldsymbol{x}_j\right|, h\right).$$

Coupling algorithm is used for the discretization of computational domains of the same material in different domains, or different materials using different computational methods. The same computational formula is applied in SPH and Lagrange.

The main difference between SPH and Lagrange is that SPH uses discrete nodes to simulate computational domain and Lagrange uses continuous elements to discretize the domain. SPH is similar to Lagrange if a SPH particle is regarded as an element with only one node. In coupling algorithm, it is necessary to define the interaction of the interface of domain using different discrete methods. The interaction algorithm in interface mainly includes kinematic constraint method, distributed parameter method and penalty method. Quite in contrast to other methods, the penalty method approach is found to excite little if any mesh hour glassing. This lack of noise is undoubtedly attributable to the symmetry of the approach. Momentum is exactly conserved without the necessity of imposing impact and release conditions. It is widely used in the numerical calculation. Therefore, the penalty method is used in the interface of SPH and Lagrange [Hallquist (2006)].

In the numerical simulation model of human-stem-tuber-soil system, large deformations occur in the inner soil, and SPH nodes of the inner soil are defined as slave nodes. Small deformations occur in the outer soil, and surface of the Lagrange element of the outer soil which contact with SPH nodes is defined as master surface. The coupling between the inner and outer soil is realized by "nodes to surface" in LS-DYNA [Wang, Gao, and Gong (2010)]. The contact between SPH and Lagrange is determined by the geometrical conditions. If contact conditions are satisfied, the contact force is determined by penalty method, and SPH particles interaction force is applied to surface of the Lagrange element.

2.2 Geometry Model

A cassava tuber system is distributed in soil as monolayer disc shape. A single tuber is similar to a long cone (figure 1). SPH method requires that all the SPH particles of the same material which have the same quality and particles in a numerical simulation model are well-distributed and regular. Therefore, in cassava model, the part of a single tuber that closes to the stem is simplified to a cuboid and the rest is a long frustum of a square pyramid. The stem is simplified into a cuboid and the tubers are in symmetric distribution. When the tubers are lifted, large deformations and fractures of the soils closed to the tubers occur and small deformations occur in most parts of the rest. Thus, Lagrange-SPH coupling algorithm is applied in the soil model. SPH method is used in inner layer soil where large deformations occur and Lagrange method is used in the outer layer soil where small deformations occur. Moreover, in order to save calculation time, under the circumstance that finite element grids are not allowed to severe mesh distortions and influent the numerical simulation calculation, modeling size of SPH should be as small as possible. And to avoid the effect of wave reflex in a boundary to solution domain, a non-reflecting boundary is applied to simulate ground in the outer

boundary of outside layer soil. Meanwhile, modeling size of Lagrange should be decreased to reduce the calculation time. According to the above requirements and growth situation of cassava, geometric dimension of solid model is determined. The length of a longish tuber is 250mm. The sectional size of the tuber close to the stem is 30mm×30mm and the length is 45mm. The sectional size of the tail end of the tuber is 10mm×10mm. The length of a shorter tuber is 200mm. The section size of the tuber close to the stem is 30mm×30mm and the length is 38mm. The sectional size of the tail end of the tuber is 10mm×10mm. The tuber system is in soil at 150mm depth. The size of the stem is 30mm×30mm×230mm. The size of soil model is 1200mm×1200mm×280mm and the size of inner layer soil is 824mm×824mm×180mm. The simplified model of cassava is shown in figure 2. Due to the symmetry of the model, a 1/4 of solid model is built.

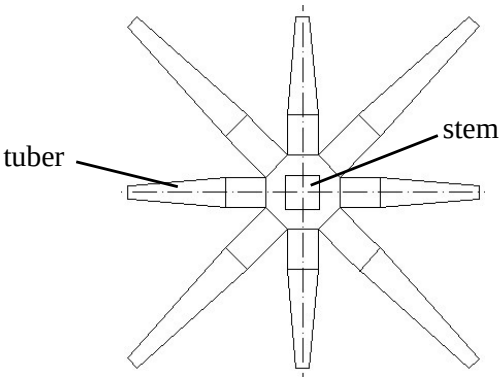

Figure 2: Simplified model of cassava.

2.3 Material model

Soil model: the constitutive relation of soil has great influence on the precision of lifting simulation results [Wu and Robert (2007); Zhong, Jiang, Jiang, Zhao, Qiao and Zhang (2010)]. In order to improve the accuracy of simulation, referring to documents [Lewis (2004)], MAT_FHWA_SOIL is selected as soil material model because it takes account of the influence of moisture content, strain softening, strain rate effect, void ratio, and pore-water pressure and obeys the modified mohr-coulomb yield criterion as follow:

$$F = -P\sin\varphi + \sqrt{J_2K^2(\theta) + A^2\sin^2\varphi} - c\cos\varphi = 0 \tag{4}$$

Where P is pressure, φ is angle of internal friction, J_2 is second invariant of the stress deviator, $K(\theta)$ is function of angle in the deviatoric plane, A is Drucker-Prager coefficient and c is cohesion.

According to test results of soil on the cultivated farm, the main material parameters of soil model are obtained: soil density is 1880 kg/m^3, bulk modulus is 0.55×10^6 Pa, shear modulus is 0.25×10^6 Pa, angle of internal friction is 10.03°, cohesion is 3kPa, and moisture content is 15%. Cassava tuber is similar to an isotropic elastic-plastic material and its stem is similar to an anisotropic elastic-plastic material [Yang, Yang, Zheng, Wang, Jia and Zhao (2011)]. Taking no account of tubers breakage and the effect of stem material parameters to the lifting procedure, for the convenience of the establishment of model, both the tuber and the stem are regarded as isotropic elastic material in this study. Material parameters of the tuber are as follow: density is 1 036 kg/m^3, elasticity modulus is 7.23×10^6 Pa, Poisson ratio is 0.3. Material parameters of stem are as follow: density is 836.8 kg/m^3, elasticity modulus is 35.36×10^6 Pa, Poisson ratio is 0.3[Yang, Yang, Zheng, Wang, Jia and Zhao (2011)].

2.4 Numerical simulation model

The element numbers of the numerical simulation model are as following: inner layer soil is 64813, outer layer soil is 78130, the stem is 152, the cuboid tuber close to the stem is 69 and the frustum of a square pyramid tuber is 66. Because only 1/4 of the solid model is discretized, the symmetrical boundary conditions are defined as following: the freedom of the grid nodes in the symmetrical boundary is constrained and the particles near the symmetrical boundary are dealt with virtual particle method [Liu and Liu (2005); Hallquist (2006)]. Meanwhile, the outer boundary of the outer layer soil is all constrained. The contact among the tuber, the stem and soil is defined as "nodes to surface" in LS-DYNA [Hallquist (2006)]. For simplifying model, the manually pulling velocity was applied on the stem directly. Numerical simulation model of human-stem-tuber-soil system is built, as shown in figure 3.

3 Results and Discussion

3.1 Model verification

Model validation was verified by comparing the lifting force on tuber obtained by field test and simulation test. The manually pulling velocity which was measured by the field test was applied in the numerical simulation test. A dynamic strain tester (DH5937, Jiangsu Donghua Testing Technology Co., LTD) was used to run the field tests. The sampling frequency was 50Hz. The force transducer consisted

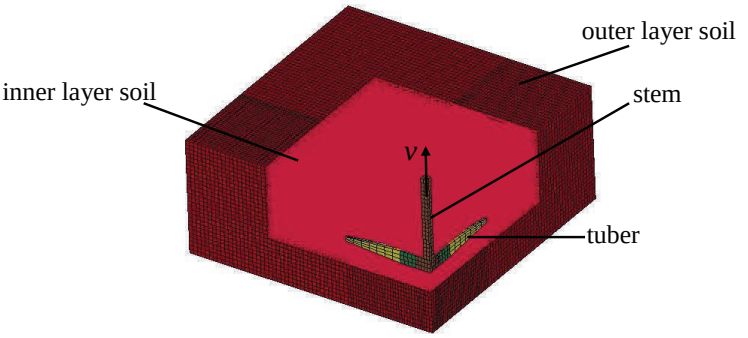

Figure 3: Numerical simulation model of human-stem-tuber-soil system.

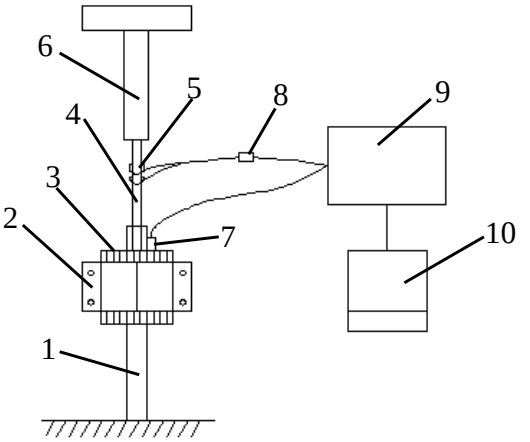

1.stem 2. cassava clamping device 3. toothed plate 4. connecting plate 5. strain gauge 6. pipe 7. acceleration sensor 8. bridge arm resistance 9. strain tester 10. notebook computer

Figure 4: Diagram of measurement system for lifting force and acceleration.

Figure 5: Test on the field.

of 4 strain gages which were stuck on the connecting plate. The measurement system for the determinations of lifting force and acceleration is shown in figure 4. The test scene is shown in Figure 5.

A full-bridge connection was selected as the bridge connection method. Force transducer was calibrated by weighing. The significance level of the regression equation of stain and weight gravity is 0.0001. The regression equation is expressed by

$$y_s = 0.0343x_g - 0.228 \tag{5}$$

Where x_g is weight gravity, y_s is stain. The relation curve is shown in figure 6.

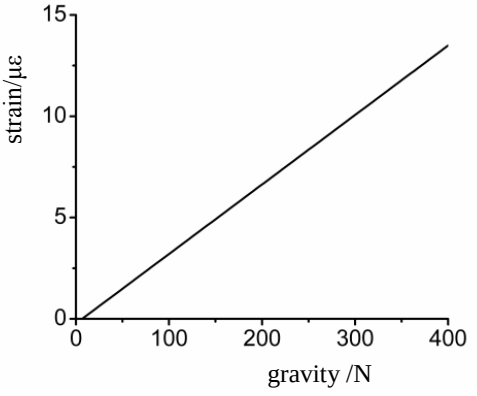

Figure 6: Relationship curve between gravity and strain.

The manually pulling velocity which was measured by the field test is expressed by

$$v = 0.051 + 0.23t + 0.08\sin(29.79t - 0.7) \tag{6}$$

The lifting forces obtained by the field test and simulation test are shown in figure 7. Figure 7 shows that value and changing trend of the measured curve and the simulated curve are basically consistent, which demonstrates that the numerical simulation model of human-stem-tuber-soil system is suitable for the numerical simulation study of lifting procedure of cassava tuber.

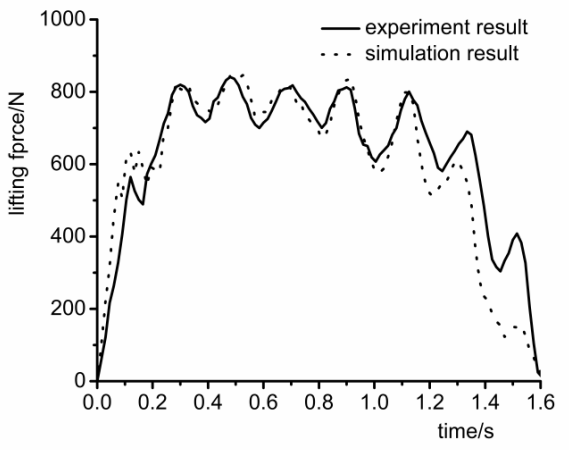

Figure 7: The comparison between physical test curve and simulated curve.

3.2 Lifting procedure of cassava tuber

The screenshot of the interaction between a tuber and soil are shown in Figure 8. Thickness of the screenshot on the vertical direction is consistent with the thickness of a tuber. Shown as figure 8a, because the size of the part of tuber close to the stem is big and the tail end of tuber is small, the bending deformation occurs at the bottom of the tuber easily, which leads to a weak extrusion to soil. Therefore, when the tuber is lifted, the extrusion of the part of tuber close to the stem to the soil is larger. Shown as figure 8b, 8c and 8d, during the continuous lifting procedure, the extrusion of the tuber to the soil and shear stress of the soil increase gradually. This is shearing the soil in truncated cone pattern. Meanwhile, due to the small size of the rear of the tuber and its weak bending resistance, the upper soil close to the stem is bended and fractured because of gravity and tensile stress. The falling fractured soil enhances the bending and the rapture of the upper soil. Shown as 8e and 8f,

due to the further lifting and jitter of the tuber, the soil is gradually detached from the tuber and falls down. The tuber gradually returns to its original state because of elastic restoring force. The screenshot also shows that the shape of disc cavity caused by the soil separation matches with the results observed in field tests.

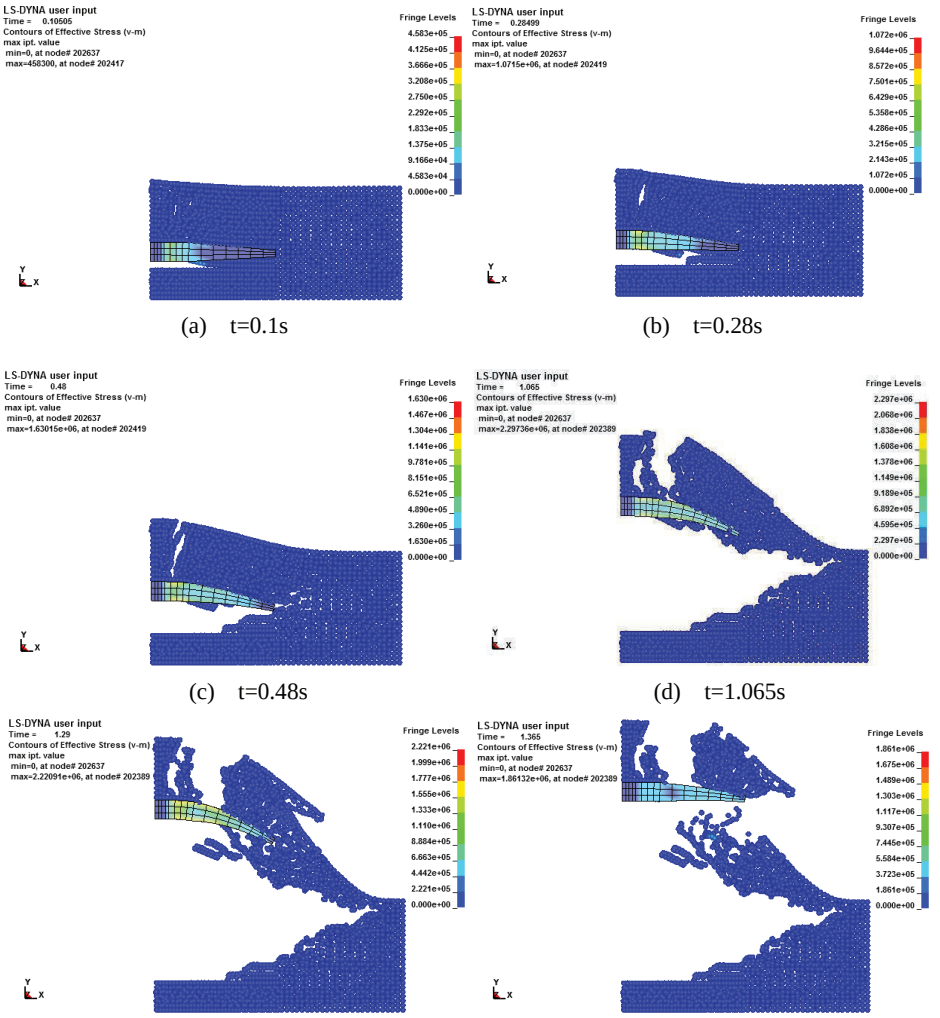

Figure 8: Numerical simulation of the lifting procedure of the cassava tuber.

3.3 Change of Tuber's Stress

The variation of tuber's effective stress during lifting procedure is shown in Figure 9. Shown as figure 9, when the tuber is uplifted, because of the increasing of the extrusion of tuber to soil, the bending deformation of the tuber and the effective stress inside the connection between tuber and stem increase gradually, and the effective stress expands from the connection along with the tuber to outside end of tuber. During this lifting period, the stress has a maximum value at the connection point. Shown as 9c, 9d, 9e and 9f, after tuber' s effective stress achieves the highest value, due to jittering of the tuber, the effective stress decreases at first and then increases. Continuous jittering on the soil helps soils fall off the tuber, resulting in the gradual decreasing of the bending deformation and the effective stress. At the end of lifting, the tuber returns to its original state because of its elastic restoring force.

3.4 Procedure of Shear Failure of Soil

The screenshots of effective stress of soil during tuber lifting procedure is shown as Figure 10. Thickness of the screenshot on the vertical direction is consistent with the thickness of a tuber. Shown as figure 10, when the tuber is lifted, the extrusion of tuber to soil increases, and the effective stress of soil on top of the tuber increases gradually. The highest soil stress is achieved where the soil clings to the tuber. At the time t=0.52s, when the soil volume was compressed by 5% in the lifting direction, at the tail end of the tuber the ring sheared surface of soil occurs. The angle between the surface and the ground is 35°. Meanwhile, because of the increasing of the extrusion of tuber to soil and the bending deformation of tuber, bending tensile stress of surface soil increases during lifting. The surface soil is bended and fractured. The further tuber lifting increases the extrusion of tuber to soil, the effective stress of soil on top of the tuber, and the soil separation along with the ring sheared surface.

When the soil is nearly separated, a further tensile fracture is enhanced due to the effect of the soil gravity. After that, the soil falls down on ground due to tuber jittering and completely detaches from the tuber.

3.5 Influence of pulling velocity

Equation (6) is a manually pulling velocity model measured by the field test. The velocity model can be superimposed by a line and a sine curve. The increasing of the velocity with time and value of the velocity are determined by the slope of the line in equation (6). And the sine curve has the greatest influence on jittering on the soil. Therefore, for the convenience of analyzing the influence of lifting velocity

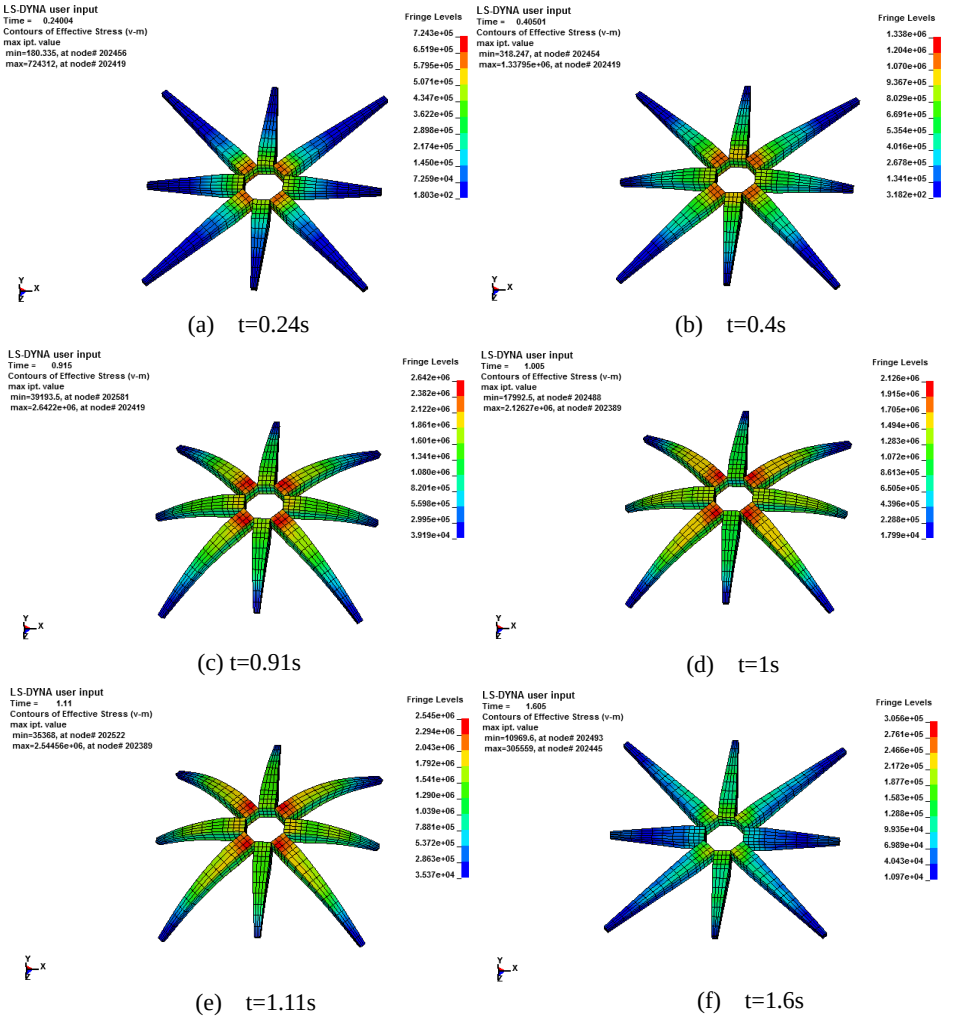

Figure 9: Effective stress of cassava tuber.

on the lifting force and effective stress of tuber and to avoid large variation in lifting velocity model, only the slope in the velocity model was changed. Based on the changed lifting velocity models, numerical simulation models were developed to carry out numerical simulations of pulling cassava tubers. According to the numerical simulation analysis of the models, influence of lifting velocity on the lifting force and effective stress of tuber was studied. In the models, the slope in lifting velocity models is 0.23, 0.55, and 0.9, respectively. The simulation results

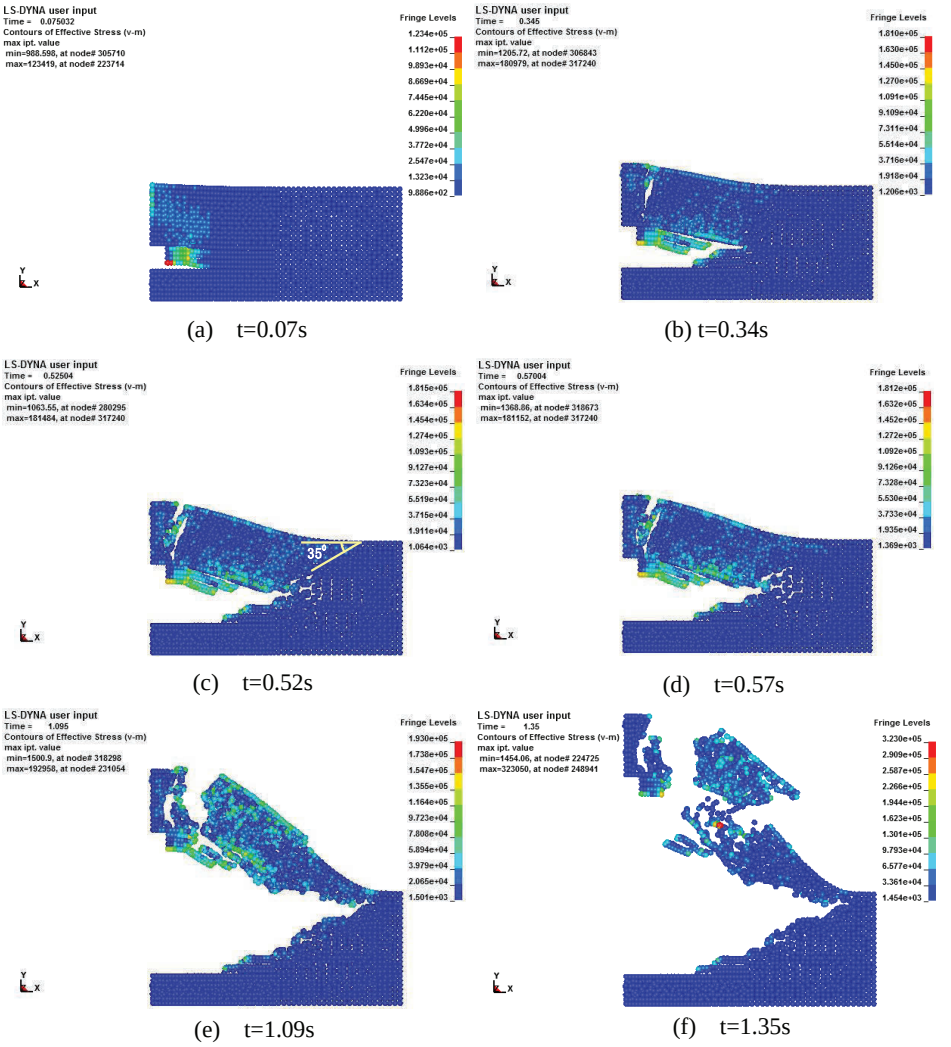

Figure 10: The effective stress of soil.

are shown in Figure 11, 12 and 13. The variation of lifting velocity with lifting height of the stem is shown in Figure 11. The variation of lifting force with lifting height of the stem is shown in Figure 12. The variation of effective stress of tuber with lifting height of the stem is shown in Figure 13.

Shown as figure 11, when the lifting height is low, the frequency of jitter is high. But the frequency decreases with the increasing of the height. And lifting velocity increases with the increasing of the slope. At the later stage of tuber lifting, the

frequency becomes lower with the increasing of the height, which was harmful to the soil detaching from tuber.

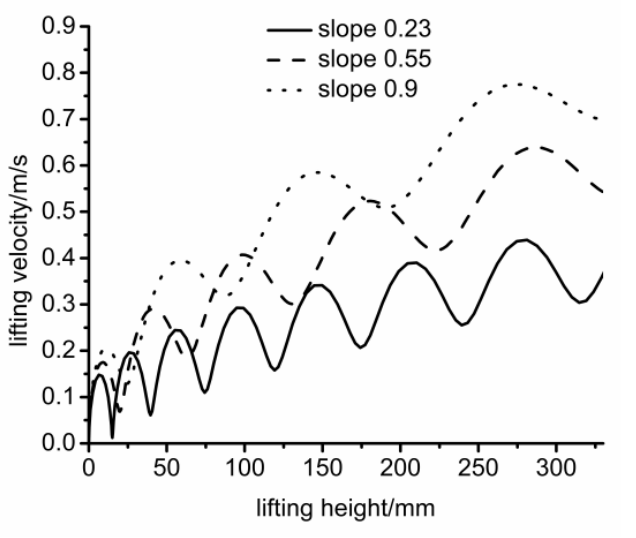

Figure 11: The variation of lifting velocity with lifting height of the stem.

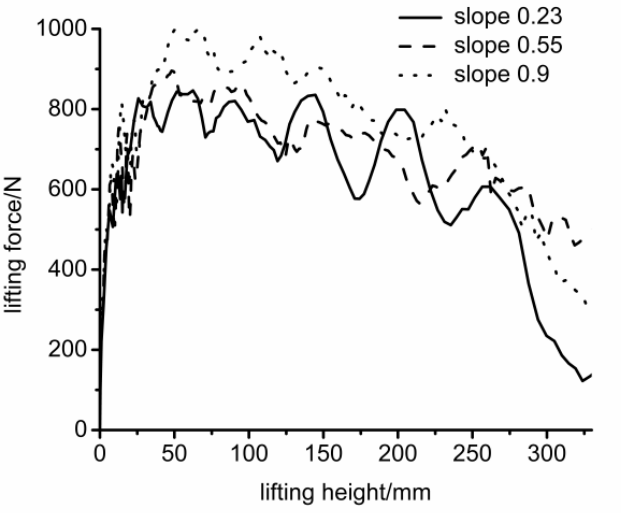

Figure 12: The variation of lifting force with lifting height of the stem.

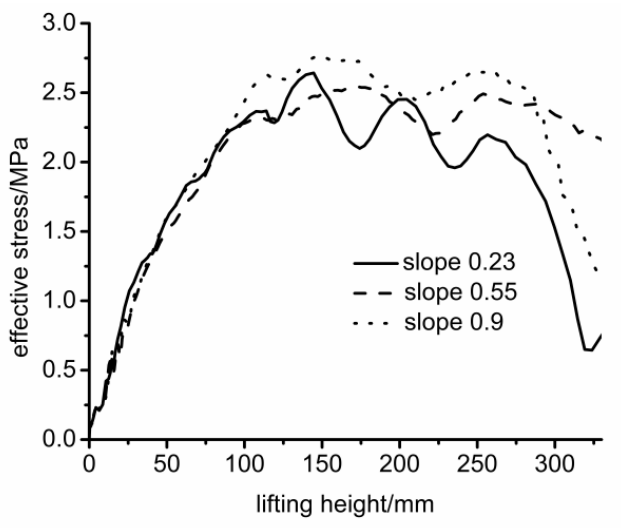

Figure 13: The variation of effective stress of tuber with lifting height of the stem.

Shown as figure 12, lifting force increases rapidly with the increasing of the lifting height at first, and then decreases gradually. When the height is 50 mm and the soil volume was compressed by 5% in the lifting direction, the lifting force achieves the highest value. The reason is that when the tuber is lifted, the extrusion of tuber to soil and lifting force increase gradually. When the height is 50 mm, shear stress of the soil is a little larger than shear strength of the soil, the ring sheared surface of soil occurs, and area of sheared soil was maximum. The lifting force achieves the highest value. After that, with the increasing of the height, the rest of the area and lifting force decreases gradually. In figure 12, maximum lifting force increases with the increasing of the slope. The reason is that lifting velocity increases with the slope, resulting in the increasing of shear strength of soil and lifting force [Yang, Cai, Yang and Huang (2011)] and high harvesting efficiency. And according to figure 12, when the height is 330 mm, consumption of energy during lifting is 207.5, 228.7, and 248.7N·m, respectively. It shows that consumption of energy increases with the increasing of lifting velocity.

Shown as figure 13, maximum effective stress of tuber doesn't increase with the increasing of lifting velocity or maximum lifting force. When the slope is 0.9, maximum effective stress of tuber is the largest, and when the slope is 0.23, the stress is smaller, and when the slope is 0.55, the stress is smallest. The reason is that due to the different lifting velocities during lifting, bending stress and shear stress inside the connection between tuber and stem are different. When the lifting

velocity is large, bending stress is small, but shear stress is large. When the lifting velocity is small, bending stress is large, but shear stress is small. And maximum effective stress of tuber is determined by the bending stress and the shear stress. Meanwhile, shown as figure 13, before the height achieves 75 mm, effective stress of the tuber is smaller. When the height is 75 mm, effective stress of the tuber is 25% smaller than of the bending strength of tuber (2.66MPa) [Yang, Yang, Zheng, Wang, Jia and Zhao (2011)]. After that, the effective stress is larger. Thus, in the design of lifting mechanism system, before the height achieves 75 mm, higher velocity is beneficial for improving harvest efficiency, but after that, lifting velocity should be appropriate to avoid too high effective stress that may result in tuber broken and lost.

Shown as figure 12 and 13, the height when maximum lifting force occurs is lower than the height when maximum effective stress of tuber occurs. The reason is that when maximum lifting force occurs, bending deformation of tuber and bending stress are smaller.

4 Conclusion

(1) The numerical simulation model of human-stem-tuber-soil system based on the coupling algorithm of Lagrange and smoothed particle hydrodynamics (SPH) is suitable for the numerical simulation study of lifting procedure of cassava tubers.

(2) There is a maximum effective stress at the connection point between the stem and a tuber due to the interaction of tuber deformation and soil deformation during lifting tubers. The tubers might be broken if the maximum effective stress was higher than the tuber strength. When a cassava tuber is lifted, the effective stress inside the connection between the tuber and the stem increases gradually, and expands gradually from the connecting point along with the tuber to the outside end of tuber. During the lifting period, the effective stress has a maximum value at the connection point. When the tuber is lifted, the extrusion of tuber to soil increases and the effective stress of soil on top of the tuber increases gradually, which result in shear fracture of soil. When the soil volume was compressed by 5% in the lifting direction, at the tail end of the tuber the ring sheared surface of soil occurs. The angle between the surface and the ground is 35^o. The soil is sheared and fractured along with the ring sheared surface gradually. After that, the soil falls down on ground due to tuber jittering and completely detaches from the tuber.

(3) High lifting velocity result in high harvesting efficiency, but consumption of energy also increases. Before the height achieves 75 mm, tuber's effective stress is comparatively small. Therefore, in the design of lifting mechanism system, before the height achieves 75 mm, higher velocity is beneficial for improving harvest

efficiency, but after that, lifting velocity should be appropriate to avoid too high effective stress that may result in tuber broken and lost.

Acknowledgement: This work was supported by a grant from the National Natural Science Foundation of China (Grant No.51365005 and Grant No.51065003) and Guangxi Key Laboratory of Manufacturing System & Advanced Manufacturing Technology (Grant No.13-051-09S01).

Reference

Agbetoye, L. A. S. (1999): Developments in Cassava Harvesting Mechanization. *West Indian Journal of Engineering*, vol. 22, no. 1, pp. 11-19.

Agbetoye, L. A. S.; Dyson, J.; Kilgour, J. (2000): Prediction of the lifting forces for cassava harvesting. *Journal of Agricultural Engineering Research*, vol. 75, no. 1, pp. 39-48.

Benz, W.; Asphaug, E. (1995): Simulations of brittle solids using smooth particle hydrodynamics. *Computer Physics Communications*, vol. 87, no. 1-2, pp. 253-265.

Bobobee, E. Y. H.; Okyere, J. B.; Twum, A.; Neumann, R. H.; Knechtges, H. (1994): Performance Evaluation of a Mechanical Cassava Harvester. Proceedings of the International Commission of Agricultural Engineering (CIGR) XII World Congress, Milano, Italy, August 29-September 1, 1994: Report No. 94-D-066. Chm-3407 Cassava Harvesting Machine. Et Moisakula Ltd, Estonia.

Campbell, J. C.; Vignjevic, R.; Patel, M.; Milisavljevic, S. (2009): Simulation of water loading on deformable structures using SPH. *CMES-Computer Modeling in Engineering & Sciences*, vol. 49, no. 1, pp. 1-21.

Caleyron, F.; Chuzel-Marmot, Y.; Combescure, A. (2009): Modeling of reinforced concrete through SPH-FE coupling and its application to the simulation of a projectile's impact onto a slab. *International Journal for Numerical Methods in Biomedical Engineering*, vol. 27, no. 6, pp. 882-898.

Cleary, P. W.; Prakash, M.; Ha, J. (2006): Novel applications of smoothed particle hydrodynamics (SPH) in metal forming. *Journal of Materials Processing Technology*, vol. 177, no. 1-3, pp. 41-48.

Dong, T. W. ; Liu, H. S.; Jiang, S. L.; Gu, L.; Xiao, Q. W.; Yu, Z.; Liu, X. F. (2013): Simulation of free surface flow with a revolving moving boundary for screw extrusion using Smoothed Particle Hydrodynamics. *CMES-Computer Modeling in Engineering & Sciences*, vol. 95, no. 5, pp. 339-360.

Fourey, G.; Oger, G.; Le Touz'e, D.; Alessandrini, B. (2010): Violent fluid-

structure interaction simulations using a coupled SPH/FEM method. *IOP Conference Series: Materials Science and Engineering*, vol. 10, no. 1, pp. 012041.

Hallquist, J. O. (2006): *LS-DYNA theory manual*. Livermore: Livermore Software Technology Corporation.

Johnson, G. R. (1994): Linking of Lagrangian particle methods to standard finite element methods for high velocity impact simulations. *Nuclear Engineering and Design*, vol. 150, no. 2-3, pp. 265-274.

Kolawole, P. O.; Agbetoye, L.; Ogunlowo, S. A. (2010): Sustaining World Food Security with Improved Cassava Processing Technology: The Nigeria Experience. *Sustainability*, vol. 2, pp. 3681-3694.

Lewis, B. A. (2004): *Manual for LS-DYNA soil material model 147*. Department of Transportation: Federal Highway Administration.

Liao, Y. L.; Sun, Y. P.; Liu, S. H.; Cheng, D. P.; Wang, G. P. (2012): Development and prototype trial of digging-pulling style cassava harvester. *Transactions of the CSAE*, vol. 28, no. Supp. 2, pp. 29-35.

Limido, J.; Espinosa, C.; Salaun, M.; Lacome, J. L. (2006): A new approach of high speed cutting modeling: SPH method. *Journal of Physics IV*, vol. 134, no. 1, pp. 1195-1200.

Liu, G. R.; Liu, M. B. (2005): *Smoothed particle hydrodynamics: A meshfree particle method*. Translated by Han Xu, Yang Gang, Qiang Hongfu. Changsha: Hunan University Press.

Lu, Y.; Wang, Z. Q.; Chong, K. (2005): A comparative study of buried structure in soil subjected to blast load using 2D and 3D numerical simulations. *Soil Dynamics and Earthquake Engineering*, vol. 25, no. 4, pp. 275-288.

Messahel , R.; Souli, M. (2013): SPH and ALE formulations for fluid structure coupling. *CMES-Computer Modeling in Engineering & Sciences*, vol. 96, no. 6, pp. 435-455.

Seo, S.; Min, O.; Lee, J. (2008): Application of an improved contact algorithm for penetration analysis in SPH. *International Journal of Impact Engineering*, vol. 35, no. 6, pp. 578-588.

Vignjevic, R.;De Vuyst, T.; Campbell, J. C. (2006): A frictionless contact algorithm for meshless methods. *CMES-Computer Modeling in Engineering & Sciences*, vol. 13, no. 1, pp. 35-47.

Wang, J. M.; Gao, N.; Gong, W. J. (2010): Abrasive waterjet machining simulation by coupling smoothed particle hydrodynamics/finite element method. *Chinese Journal of Mechanical Engineering*, vol. 23, no. 5, pp. 568-573.

Wu, W. J.; Robert, T. (2007): A study of the interaction between a guardrail post

and soil during quasi-static and dynamic loading. *International Journal of Impact Engineering*, vol. 34, no. 5, pp. 883–898.

Yang, W.; Cai, G. W.; Yang, J.; Huang, Y. Q. (2011): Mechanical and mathematical model analysis of uprooted force on cassava storage root. *Transactions of the CSAE*, vol. 27, no. 11, pp. 95-100.

Yang, W.; Yang, J.; Zheng, X. T.; Wang, Q. Y.; Jia, F. Y.; Zhao, J. Q. (2011): Experiment on mechanical properties of cassava. *Transactions of the CSAE*, vol. 27, no. (Suppl.2), pp. 50-54.

Yang, W.; Yang, J.; Jia, F. Y.; Wang, Q. Y.; Huang, Y. Q. (2013): Numerical simulation of digging operation of cassava root planted in red clay. *Journal of Mechanical Engineering*, vol. 49, no. 9, pp. 135-143.

Zhang, Z. C.; Qiang, H. F.; Gao, W. R. (2011): Coupling of smoothed particle hydrodynamics and finite element method for impact dynamics simulation. *Engineering Structures*, vol. 33, no. 1, pp. 255–264.

Zhong, J.; Jiang, J. D.; Jiang, T.; Zhao, Z. F.; Qiao, X.; Zhang, X. (2010): Deep-tillage rotavator technology based on smoothed particle hydrodynamics simulation. *Journal of Mechanical Engineering*, vol. 46, no. 19, pp. 63-69.